Available online at www.sciencedirect.com
SCIENCE DIRECT®
Inorganica Chimica Acta 357 (2004) 3532–3540
Inorganica Chimica Acta
www.elsevier.com/locate/ica

Structures of sulfur-rich dithiolate-gold(I) complexes and their oxidation

Tatsuya Ryowa, Motohiro Nakano, Hatsue Tamura, Gen-etsu Matsubayashi *

Department of Molecular Chemistry and Frontier Research Center, Graduate School of Engineering, Osaka University, 1-16, Machikaneyama, Toyonaka, Osaka 560-0043, Japan

Received 14 January 2004; accepted 5 March 2004
Available online 19 May 2004

Abstract

$[NMe_4][Au(PEt_3)(C_3S_5)]$, $[NMe_4][Au(PPh_3)(C_3S_5)]$, $[NMe_4][Au(PEt_3)(C_8H_4S_8)]$, [*N*-methylpyridinium]$[Au(PPh_3)(C_8H_4S_8)]$, $[(PEt_3)Au–C_3S_5–Au(PEt_3)]$, and $[(PEt_3)Au–C_8H_4S_8–Au(PEt_3)]$ [$C_3S_5^{2-}$ = 4,5-disulfanyl-1,3-dithiole-2-thionate(2−); $C_8H_4S_8^{2-}$ = 2-{(4,5-ethylenedithio)-1,3-dithiole-2-ylidene}-1,3-dithiole-4,5-dithionate(2−)] were prepared. They exhibited first oxidation potentials due to the dithiolate ligand-centered oxidation at −0.30 to +0.21 V (vs. Ag/Ag^+) in dichloromethane. They were reacted with iodine or 7,7,8,8-tetracyano-*p*-quinodimethane (TCNQ) to afford one-electron-oxidized species $[Au(PEt_3)(C_8H_4S_8)]$ and $[(L)Au–C_8H_4S_8–Au(L)](TCNQ)_{1.0–1.1}$, (L = PEt_3 and PPh_3) and further-electron-oxidized species $[Au(PEt_3)(S–S)]I_{3.3–5.7}$, $[Au(PPh_3)(S–S)]I_{12–13}$, $[(PEt_3)Au–(S–S)–Au(PEt_3)]I_{3.3–5.5}$ (S–S = $C_3S_5^{2-}$ and $C_8H_4S_8^{2-}$) and $[(PPh_3)Au–C_8H_4S_8–Au(PPh_3)]I_{12}$. ESR spectra of the oxidized species suggest the C_3S_5 and $C_8H_4S_8$ ligand-centered oxidation. The oxidized $C_8H_4S_8$-complexes showed electrical conductivities of 10^{-4}–10^{-2} $S\,cm^{-1}$ measured for compacted pellets at room temperature. X-ray crystal structures of $[NMe_4][Au(PPh_3)(C_3S_5)]CH_2Cl_2$, $[(PEt_3)Au–C_3S_5–Au(PEt_3)]$ and $[(PEt_3)Au–C_8H_4S_8–Au(PEt_3)]$ were revealed.
© 2004 Elsevier B.V. All rights reserved.

Keywords: Gold complexes; Dithiolate complexes; Crystal structures; Electrical conductivity

1. Introduction

Many metal complexes with sulfur-rich dithiolate ligands, $C_3S_5^{2-}$ [4,5-disulfanyl-1,3-dithiole-2-thionate(2−)] (**A**) [1–4] and $C_8H_4S_8^{2-}$ [2-{(4,5-ethylenedithio)-1,3-dithiole-2-ylidene}-1,3-dithiole-4,5-dithionate(2−)] (**B**) [4], have been studied extensively as good electrical conductors including some superconductors. The latter dithiolate ligand having more sulfur atoms as a further extended π-electron system forms a stable oxidized state, and even bulky metal complexes with this ligand construct good electron-conduction pathways through many non-bonded S–S contacts in the solid state [4–7].

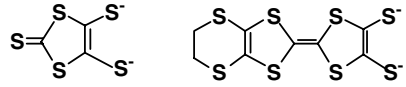

A **B**

Gold(III) complexes with the sulfur-rich dithiolate ligands having a planar geometry behave as good electrical conductors [8–12]. On the other hand, gold(I) complexes with dithiolate ligands are known to have two- and/or three-coordinate geometries, together with further Au–S and Au–Au interactions [13–15], and some complexes with the C_3S_5 ligand were prepared and structurally studied [16–18]. However, the oxidized species of the sulfur-rich dithiolate gold(I) complexes have not been fully studied. Thus, gold(I) complexes with the $C_8H_4S_8$ ligand are expected to afford good electrical conductors having unique molecular interactions and packings in the solid state.

This paper reports preparations of anionic complexes of the $[Au(PR_3)(C_8H_4S_8)]^-$ type and neutral dinuclear species $[Au(PR_3)–C_8H_4S_8–Au(PR_3)]$ (R = Et and Ph) as

* Corresponding author. Tel.: +81-6-6850-5769; fax: +81-6-6850-5785.
E-mail address: matsu@ch.wani.osaka-u.ac.jp (G. Matsubayashi).

0020-1693/$ - see front matter © 2004 Elsevier B.V. All rights reserved.
doi:10.1016/j.ica.2004.03.048

well as the corresponding C_3S_5-complexes, and their oxidation and electrical conductivities of the oxidized species. The crystal structures of $[NMe_4][Au(PPh_3)(C_3S_5)]$, $[(PEt_3)Au–C_3S_5–Au(PEt_3)]$ and $[(PEt_3)Au–C_8H_4S_8–Au(PEt_3)]$ are also described.

2. Experimental

2.1. Materials

4,5-Bis(cyanoethylthio)-1,3-dithiole-2-thione, $C_3S_5(CH_2CH_2CN)_2$ [19], and 4,5-bis-(cyanoethylthio)-1,3-dithiole-2-[(4,5-ethylenedithio)-1,3-dithiole-2-ylidene], $C_8H_4S_8(CH_2CH_2CN)_2$ [20–22], as pro-ligand compounds of $C_3S_5^{2-}$ and $C_8H_4S_8^{2-}$ dithiolates, were prepared according to the literatures. (Triethylphosphine) chlorogold(I), (triphenylphosphine)chlorogold(I) $[AuCl(PR_3)]$ (R = Et and Ph), and 7,7,8,8-tetracyano-*p*-quinodimethane (TCNQ) were commercially available.

2.2. Preparations of $[NMe_4][Au(PR_3)(C_3S_5)]$ [R = Et (**1**) and Ph (**2**)]

All the following reactions were performed under an argon atmosphere. To an ethanol (30 cm^3) solution of $C_3S_5(CH_2CH_2CN)_2$ (280 mg, 0.90 mmol) was added with vigorous stirring a methanol (3.6 g, 25 wt%) solution containing NMe_4OH (900 mg, 9.8 mmol) and the solution was stirred for 15 min. To the solution was added with stirring a methanol (20 cm^3) solution of $AuCl(PEt_3)$ (350 mg, 0.98 mmol) and the solution was stirred for 30 min at room temperature. The resulting red solids of **1** were collected by filtration, washed with methanol, and dried in vacuo (60% yield). *Anal.* Calc. for $C_{13}H_{27}AuNPS_5$: C, 26.66; H, 4.65; N, 2.39. Found: C, 26.19; H, 4.37; N, 2.58%. ^1H NMR (in $CDCl_3$): δ 3.21 (12H, s, NMe_4^+), 1.77 (6H, m, CH_2), 1.20 (9H, m, CH_3).

Similarly, an ethanol (30 cm^3) solution of $[NMe_4]_2[C_3S_5]$ prepared by the reaction of $C_3S_5(CH_2CH_2CN)_2$ (280 mg, 0.90 mmol) with NMe_4OH (900 mg, 9.8 mmol) was reacted with a dichloromethane (20 cm^3) solution of $AuCl(PPh_3)$ (490 mg, 1.0 mmol) to yield red solids of **2** (60% yield). *Anal.* Calc. for $C_{25}H_{27}AuNPS_5$: C, 41.15; H, 3.73; N, 1.92. Found: C, 40.95; H, 3.73; N, 2.02%. ^1H NMR (in DMSO-d_6): δ 3.09 (12H, s, NMe_4^+), 7.52 (15H, m, Ph). The complex was recrystallized from dichloromethane to afford orange plates of $[NMe_4][Au(PPh_3)(C_3S_5)]CH_2Cl_2$, which were suitable for the X-ray crystal structure analysis.

2.3. Preparations of $[NMe_4][Au(PEt_3)(C_8H_4S_8)]$ (**3**) and [N-methylpyridinium]$[Au(PPh_3)(C_8H_4S_8)]$ (**4**)

As described for the preparation of **1**, an ethanol (30 cm^3) solution of $[NMe_4]_2[C_8H_4S_8]$ prepared by the reaction of $C_8H_4S_8(CH_2CH_2CN)_2$ (460 mg, 1.0 mmol) with NMe_4OH (900 mg, 9.8 mmol) was reacted with a methanol (20 cm^3) solution of $AuCl(PEt_3)$ (350 mg, 1.0 mmol) immediately to yield brown solids of **3** (70% yield). *Anal.* Calc. for $C_{18}H_{31}AuNPS_8$: C, 28.98; H, 4.19; N, 1.88. Found: C, 28.75; H, 4.07; N, 2.05%. ^1H NMR (in DMSO-d_6): δ 1.07 (9H, m, CH_3), 1.68 (6H, m, CH_2), 3.10 (12H, s, NMe_4^+), 3.25 (4H, s, CH_2).

$C_8H_4S_8(CH_2CH_2CN)_2$ (460 mg, 1.0 mmol) was dissolved in an ethanol (30 cm^3) solution containing Na metal (73 mg, 3.1 mmol). To the resulting solution of $Na_2[C_8H_4S_8]$ was added with stirring a dichloromethane (10 cm^3) solution of $AuCl(PPh_3)$ (490 mg, 1.0 mmol) and *N*-methylpyridinium chloride (155 mg, 1.5 mmol), and the solution was stirred for 30 min. A brown precipitate of **4** obtained was collected by filtration, washed with dichloromethane and methanol, and dried in vacuo (70% yield). *Anal.* Calc. for $C_{32}H_{27}AuNPS_8$: C, 42.23; H, 2.99; N, 1.54. Found: C, 41.12; H, 3.03; N, 1.64%. ^1H NMR (in DMSO-d_6): δ 3.37 (3H, s, CH_3), 7.50 (15H, m, Ph), 8.12 (2H, t, CH), 8.56 (1H, t, CH), 8.98 (2H, d, CH).

2.4. Preparation of $[(PEt_3)Au–C_3S_5–Au(PEt_3)]$ (**5**)

$C_3S_5(CH_2CH_2CN)_2$ (300 mg, 1.0 mmol) was dissolved in an ethanol (30 cm^3) solution containing sodium ethanolate (Na, 120 mg, 5.0 mmol). To the resulting solution of $Na_2[C_3S_5]$ was added with stirring a methanol (15 cm^3) solution of $AuCl(PEt_3)$ (700 mg, 2.0 mmol) and the solution was stirred for 30 min. The orange precipitate of **5** obtained was collected by filtration, washed with dichloromethane and methanol, and dried in vacuo (60% yield). *Anal.* Calc. for $C_{15}H_{30}Au_2P_2S_5$: C, 21.80; H,3.66. Found: C, 21.81; H, 3.47%. ^1H NMR (in $CDCl_3$): δ 1.22 (18H, m, CH_3), 1.84 (12H, m, CH_2). The complex was recrystallized from dichloromethane to afford brown prisms of **5**, which were suitable for the X-ray analysis.

2.5. Preparations of $[(PR_3)Au–C_8H_4S_8–Au(PR_3)]$ (R = Et (**6**) and Ph (**7**))

As described for the preparation of **5**, an ethanol (30 cm^3) solution of $Na_2[C_8H_4S_8]$ prepared by the reaction of $C_8H_4S_8(CH_2CH_2CN)_2$ (460 mg, 1.0 mmol) with Na metal (120 mg, 5.0 mmol) was reacted with a methanol (20 cm^3) solution of $AuCl(PEt_3)$ (700 mg, 2.0 mmol) to afford orange solids of **6**. They were collected by filtration, washed with methanol, and dried in vacuo (70% yield). *Anal.* Calc. for $C_{20}H_{34}Au_2P_2S_8$: C, 24.34; H, 3.47. Found: C, 24.18; H, 3.12%. ^1H NMR (in $CDCl_3$): δ 1.22 (18H, m, CH_3), 1.83 (12H, m, CH_2), 3.26 (4H, s, CH_2). The complex was recrystallized from dichloromethane to afford orange blocks of **6**, which were suitable for the X-ray analysis.

Similarly, an ethanol (30 cm^3) solution of $Na_2[C_8H_4S_8]$ prepared by the reaction of $C_8H_4S_8$

$(CH_2CH_2CN)_2$ (460 mg, 1.0 mmol) with Na metal (120 mg, 5.0 mmol) was reacted with a dichloromethane (10 cm^3) solution of $AuCl(PPh_3)$ (980 mg, 2.0 mmol) to give yellow solids of **7**. They were collected by filtration, washed with ethanol, and dried in vacuo (75% yield). *Anal.* Calc. for $C_{44}H_{34}Au_2P_2S_8$: C, 41.44; H, 2.69. Found: C, 41.18; H, 2.59%. ^1H NMR (in DMSO-d_6): δ 3.28 (4H, s, CH_2), 7.43 (30H, m, Ph).

2.6. Preparations of the oxidized species (8–11) of 1–4

To a dichloromethane (30 cm^3) solution of **1** (60 mg, 0.10 mmol) was added with stirring a dichloromethane (20 cm^3) solution of iodine (130 mg, 0.50 mmol) at room temperature, immediately affording black microcrystals of $[Au(PEt_3)(C_3S_5)]I_{3.3}$ (**8**). They were collected by filtration, washed with dichloromethane, and dried in vacuo (50% yield). *Anal.* Calc. for $C_9H_{15}AuI_{3.3}S_5$: C, 11.62; H, 1.63. Found: C, 11.68; H, 1.90%.

Similarly, to dichloromethane (30 cm^3) solutions of **2**, **3**, and **4** (0.10 mmol) was added with stirring a dichloromethane (20 cm^3) solution of iodine (130 mg, 0.50 mmol) at room temperature, immediately affording black microcrystals of $[Au(PPh_3)(C_3S_5)]I_{13}$ (**9**), $[Au(PEt_3)(C_8H_4S_8)]I_{5.1}$ (**10**), and $[Au(PPh_3)(C_8H_4S_8)]I_{12}$ (**11**), respectively. They were collected by filtration, washed with dichloromethane, and dried in vacuo (55%, 50% and 60% yields). *Anal.* Calc. for $C_{21}H_{15}AuI_{13}PS_5$ (**9**): C, 11.01; H, 0.66. Found: C, 11.06; H, 0.46%. *Anal.* Calc. for $C_{14}H_{19}AuI_{5.1}PS_8$ (**10**): C, 12.75; H, 1.45. Found: C, 12.78; H, 1.12%. *Anal.* Calc. for $C_{26}H_{19}AuI_{12}PS_8$ (**11**): C, 13.35; H, 0.82. Found: C, 13.47; H, 0.88%.

2.7. Preparations of the oxidized species (12–14) of 5–7

As described for the oxidized species **8**, to dichloromethane (30 cm^3) solutions of **5**, **6** and **7** (0.10 mmol) was added with stirring a dichloromethane (20 cm^3) solution of iodine (130 mg, 0.50 mmol) at room temperature, immediately affording black microcrystals of $[(PEt_3)Au–C_3S_5–Au(PEt_3)]I_{3.3}$ (**12**), $[(PEt_3)Au–C_8H_4S_8–Au(PEt_3)]I_{5.5}$ (**13**), and $[(PPh_3)Au–C_8H_4S_8–Au–(PPh_3)]I_{12}$ (**14**), respectively. They were collected by filtration, washed with dichloromethane, and dried in vacuo (50%, 60% and 65% yields). *Anal.* Calc. for $C_{15}H_{30}Au_2I_{3.3}P_2S_5$ (**12**): C, 14.47; H, 2.43. Found: C, 14.54; H, 2.16%. *Anal.* Calc. for $C_{20}H_{34}Au_2I_{5.7}P_2S_8$ (**13**): C, 14.05; H, 2.00. Found: C, 14.00; H, 1.65%. *Anal.* Calc. for $C_{44}H_{34}Au_2I_{12}P_2S_8$ (**14**): C, 18.89; H, 1.22. Found: C, 18.70; H, 1.20%.

2.8. Preparations of the one-electron-oxidized species (15–17) of 3, 6 and 7

To an acetonitrile (30 cm^3) solution of **3** (75 mg, 0.10 mmol) was added with stirring an acetonitrile (20 cm^3) solution of TCNQ (20 mg, 0.10 mmol) at room temperature, immediately affording black microcrystals of $[Au(PEt_3)(C_8H_4S_8)]$ (**15**). They were collected by filtration, washed with acetonitrile, and dried in vacuo (60% yield). *Anal.* Calc. for $C_{14}H_{19}AuPS_8$: C, 25.03; H, 2.85. Found: C, 24.58; H, 2.55%.

To dichloromethane (30 cm^3) solutions of **6** and **7** (100 and 130 mg, respectively, 0.10 mmol) was added with stirring a dichloromethane (20 cm^3) solution of TCNQ (20 mg, 0.10 mmol) at room temperature. The solutions were added to dichloromethane (300 cm^3) and the resulting solutions were filtered through a silica gel column, which were eluted by acetonitrile. Concentration of the filtrates afforded black microcrystals of $[(PEt_3)Au–C_8H_4S_8–Au(PEt_3)](TCNQ)_{1.0}$ (**16**) and $[(PPh_3)Au–C_8H_4S_8–Au(PPh_3)](TCNQ)_{1.1}$ (**17**), respectively, which were washed with dichloromethane, collected by filtration, and dried in vacuo (50% and 60% yields, respectively). *Anal.* Calc. for $C_{32}H_{38}Au_2N_4P_2S_8$ (**16**): C, 32.28; H, 3.22; N, 4.92. Found: C, 31.83; H, 3.21; N, 4.94%. *Anal.* Calc. for $C_{57.2}H_{38.4}Au_2N_{4.4}P_2S_8$ (**17**): C, 45.80; H, 2.58; N, 4.11. Found: C, 46.40; H, 3.00; N, 4.49%.

2.9. Physical measurements

IR, electronic absorption, ESR [23] and powder reflectance spectra [24] were recorded as described previously. ^1H NMR and Raman spectra were also measured as measured previously [25]. Cyclic voltammograms of the complexes in dichloromethane were measured using $[NBu_4][ClO_4]$ as an electrolyte [26]. Electrical resistivities of the complexes were measured for compacted pellets by the conventional two-probe method at room temperature [26].

2.10. Crystal structure determination of $[NMe_4][Au(PPh_3)(C_3S_5)]CH_2Cl_2$ (2), $[(PEt_3)Au–C_3S_5–Au(PEt_3)]$ (5) and $[(PEt_3)Au–C_8H_4S_8–Au(PEt_3)]$ (6)

Intensity data were collected on a Rigaku RAXIS-RAPID imaging plate diffractometer at the Graduate School of Science, Osaka University, with graphite-monochromated Mo Kα radiation ($\lambda = 0.71069$ Å). Crystal data and details of measurements for complexes **2**, **5** and **6** are summarized in Table 1. For the data collection up to $2\theta = 55.0°$, two sets of exposures ($\phi = 0.0°$, $\chi = 45.0°$ and $\omega = 130.0$–$190.0°$; $\phi = 180.0°$, $\chi = 45.0°$ and $\omega = 0.0$–$160.0°$) were measured by scans of 3° in ω for **2** and 2° in ω for **5** and **6**. The intensity data were processed using the PROCESS-AUTO program package and corrected for Lorentz and polarization effects as well as absorption by Higashi method [27] (transmission factors, 0.387–0.594 for **2**, 0.170–0.779 for **5** and 0.232–352 for **6**). Cell constants were obtained by least-squares refinement of 26 241 ($4.5° < 2\theta < 55.0°$) for **2**, 45 086 ($4.4° < 2\theta < 55.0°$) for **5** and 40 267 ($3.3° < 2\theta < 54.9°$) reflections for **6**.

Table 1
Crystallographic data for $[NMe_4][Au(PPh_3)(C_3S_5)]CH_2Cl_2$ (**2**), $[(PEt_3)Au–C_3S_5–Au(PEt_3)]$ (**5**), and $[(PEt_3)Au–C_8H_4S_8–Au(PEt_3)]$ (**6**)

	2	**5**	**6**
Empirical formula	$C_{26}H_{29}AuCl_2NPS_5$	$C_{15}H_{30}Au_2P_2S_5$	$C_{20}H_{34}Au_2P_2S_8$
M	814.69	826.62	986.91
Crystal system	monoclinic	monoclinic	monoclinic
Space group	$P2_1/c$	$P2_1/a$	$P2_1/n$
a (Å)	17.8118(9)	13.7778(4)	13.1754(3)
b (Å)	8.6513(4)	29.9154(8)	12.5040(3)
c (Å)	20.6280(9)	13.4518(4)	18.9171(3)
β (°)	93.077(2)	117.471(1)	104.731(1)
V (Å^3)	3174.1(2)	4919.2(2)	3014.1(1)
Z	4	8	4
D_{calc} (g cm^{-3})	1.705	2.232	2.175
T (K)	296	223	283
μ (mm^{-1})	5.20	12.47	10.40
Reflection collected	14 882	16 761	13 117
Independent reflections	7238	10 734	6891
R, *wR* (all data)	0.048, 0.064	0.066, 0.091	0.032, 0.052

The structure was solved by direct methods using SHELXS86 [28] or SIR92 [29] and refined on F^2 by the full matrix least-squares technique with SHELXL97 [30]. The positions of other hydrogen atoms were geometrically calculated and refined with isotropic thermal parameters riding on those of the parent atoms. For **6**, all three ethyl moieties of one PEt_3 ligand are disordered over two sites for each ethyl group. Calculations were performed on an SGI-O2 workstation at the Graduate School of Science, Osaka University. Atomic scattering factors were taken from the usual sources [31]. Figs. 1–3 were drawn with a local version of ORTEP II [32].

3. Results and discussion

*3.1. Crystal structures of $[NMe_4][Au(PPh_3)(C_3S_5)]CH_2Cl_2$ (**2**), $[(PEt_3)Au–C_3S_5–Au(PEt_3)]$ (**5**), and $[(PEt_3)Au–C_8H_4S_8–Au(PEt_3)]$ (**6**)*

The molecular structure of the anion of complex **2** and the association of two anion moieties in the crystal are shown in Fig. 1, together with the atom-labeling scheme. Selected bond distances and angles of the anion moiety are listed in Table 2. Au, P, S(1) and S(5) atoms of the tri-coordinate anion moiety are almost coplanar

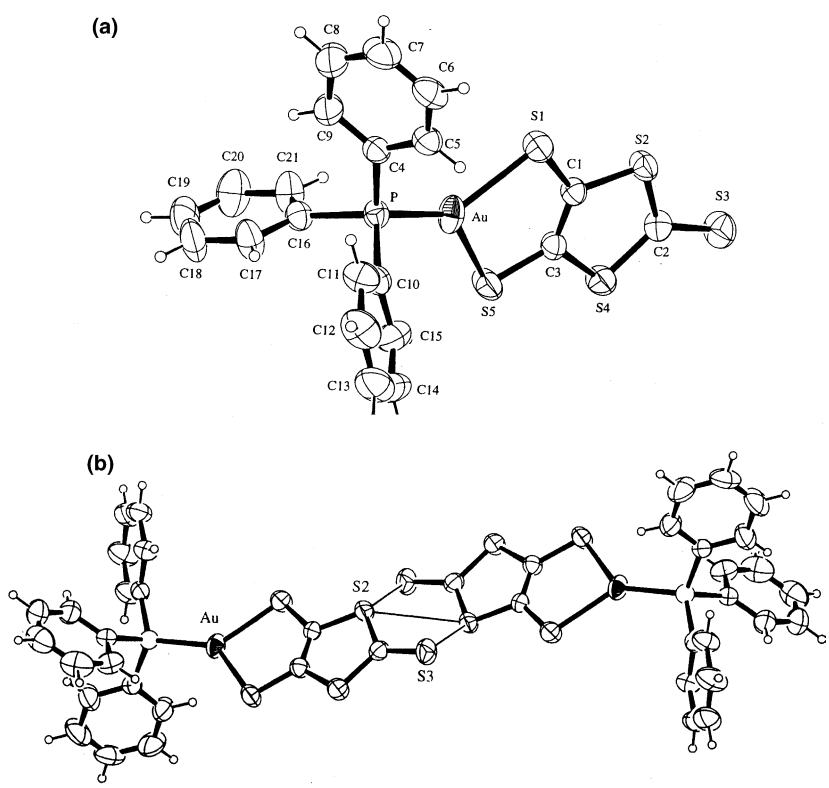

Fig. 1. (a)Geometry of the anion of $[NMe_4][Au(PPh_3)(C_3S_5)]CH_2Cl_2$ (**2**) together with the atom-labeling scheme and (b) sulfur–sulfur contacts (<3.7 Å).

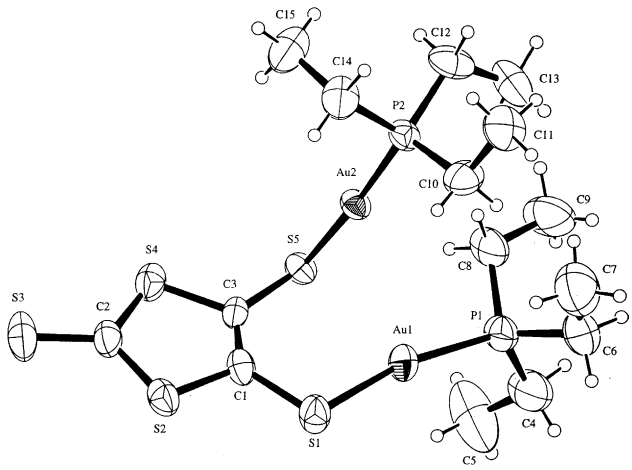

Fig. 2. Molecular structure of one molecule of two independent ones of $[(PEt_3)Au–C_3S_5–Au(PEt_3)]$ (**5**) with the atom-labeling scheme.

(±0.001 Å). Au–S [2.4544(10) and 2.4315(9) Å] and Au–P distances [2.227(9) Å], as well as the S(1)–Au–S(5) angle [89.13(3)°] are very similar to those of the anion moiety of $[NBu^n_4][Au(PPh_3)(C_3S_5)]$ [17]. In the present complex, however, two anion moieties form a dimer with S–S contacts: S(2)–S(2′), 3.520(2) and S(2)–S(3′), 3.698(2) Å. This is in contrast to the isolated anion moiety of $[NBu^n_4][Au(PPh_3)(C_3S_5)]$. The small cation moiety for the present complex may assist an effective packing leading to the anion–anion association.

The crystal structure of **5** consists of two independent molecules having almost the same geometries, and the molecular structure of one of them is shown in Fig. 2, together with the atom-labeling scheme. Since the ethyl groups bonded to the P(2) atom of **6** are disordered in two portions for each ethyl group. The molecular structure of **6** with the ethyl groups in one portion is

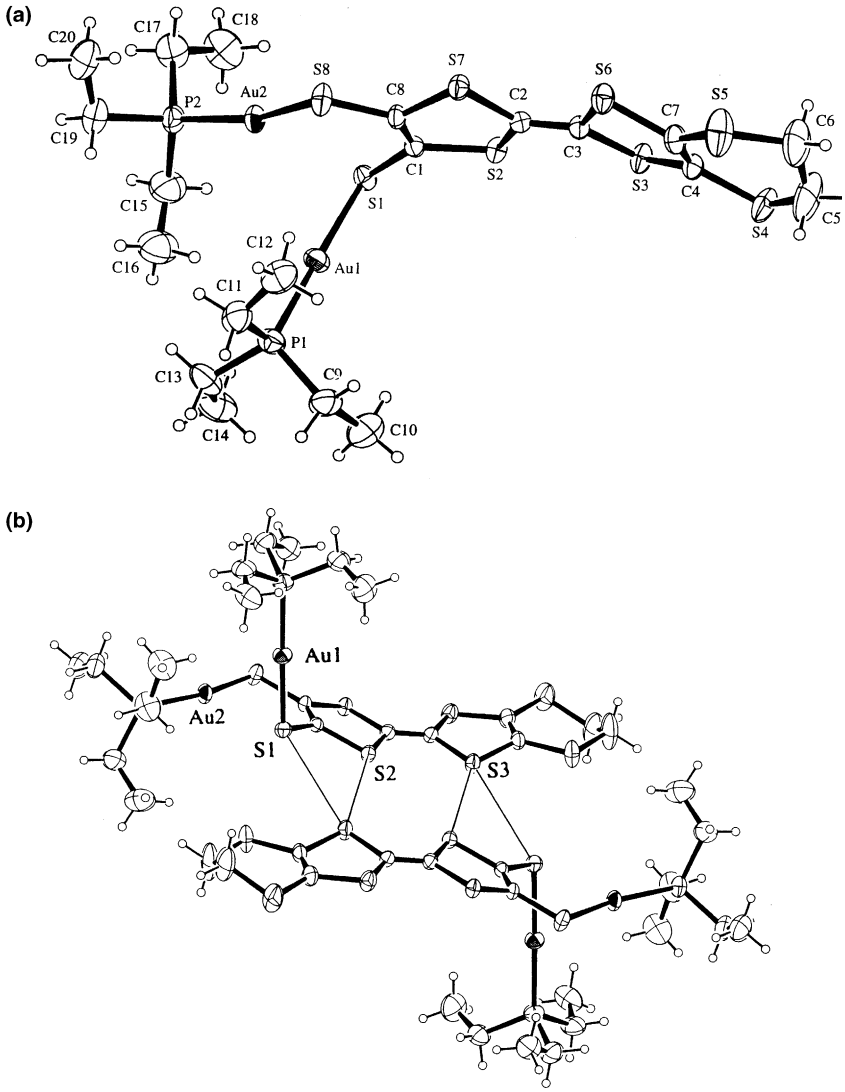

Fig. 3. (a) Molecular structure of $[(PEt_3)Au–C_8H_4S_8–Au(PEt_3)]$ (**6**) with the atom-labeling scheme and (b) sulfur–sulfur contacts (<3.7 Å). The Et groups at P(2) are disordered over two sites. Only one of the two orientations is shown.

Table 2
Selected bond distances (Å) and angles (°) of $[NMe_4][Au(PPh_3)(C_3S_5)]CH_2Cl_2$ (**2**)

Au–S(1)	2.4544(10)	Au–S(5)	2.4315(9)
Au–P	2.2427(9)	S(1)–C(1)	1.733(3)
S(2)–C(1)	1.750(3)	S(2)–C(2)	1.723(3)
S(3)–C(2)	1.652(3)	S(4)–C(2)	1.727(4)
S(4)–C(3)	1.755(3)	S(5)–C(3)	1.737(3)
C(1)–C(3)	1.356(4)		
S(1)–Au–S(5)	89.13(3)	S(1)–Au–P	134.92(3)
S(5)–Au–P	135.75(3)	Au–S(1)–C(1)	98.65(11)
Au–S(5)–C(3)	98.74(11)	C(1)–S(2)–C(2)	99.08(16)
C(2)–S(4)–C(3)	98.92(16)	S(1)–C(1)–C(3)	115.4(2)
S(2)–C(1)–C(3)	115.4(2)	S(2)–C(2)–S(4)	111.5(2)
S(2)–C(2)–S(3)	124.0(2)	S(5)–C(3)–C(1)	115.1(2)
S(5)–C(3)–C(1)	127.1(2)		

shown in Fig. 3, with the atom-labeling scheme. Selected bond distances and angles for them are given in Tables 3 and 4. For these complexes two Au atoms are bridged by C_3S_5 and $C_8H_4S_8$ ligands, respectively, bonded through the sulfur atoms. Each gold(I) center is coordinated to a PEt_3 unit. The coordination about one Au atom is approximately linear; S(5)–Au(2)–P(2), 175.64(7), S(5′)–Au(2′)–P(2′), 177.08(8)° for **5** and S(1)–Au(1)–P(1), 178.98(4)° for **6**. However, the coordination about the other Au atom is somewhat bent through an interaction between Au and S atoms; Au(1)–S(5), 2.8481(19), Au(1′)–S(5′), 2.890(2) Å and S(2)–Au(1)–P(2), 168.18(8), S(2′)–Au(1′)–P(2′), 163.35(8)° for **5**, and Au(2)–S(1), 2.9021(10) Å and S(8)–Au(2)–P(2), 164.47(4)° for **6**. The Au–S [2.320(10), 2.337(2), 2.305(2), 2.327(2) Å for **5** and 2.3389(10), 2.3403(9) Å for **6**] and Au–P bonds [2.261(2), 2.265(2), 2.254(2), 2.261(2) Å for **5**, and 2.2623(10), 2.2702(10) Å for **6**] are very close to the corresponding bonds of $[(PPh_3)Au–C_3S_5–Au(PPh_3)]$ previously reported [17]. These findings observed for the molecular structures are similar to those of gold(I)-dithiolate complexes, $[Au_2(S_2C_6H_4)(PPh_3)_2]$ [33], $[Au_2(3,4\text{-}S_2C_6H_3CH_3)(PPh_3)_2]$ [34] and $[Au_2\{S_2C_2–(CN)_2\}(PPh_3)_2]$ (R = Me, Et, OPh, Ph and cyclohexyl) [33,35].

For complex **5** there are no significant S–S contacts among the molecules in the crystal, while **6** has some S–S contacts between the molecules to form a dimeric unit: S(1)–S(6'), 3.791 and S(2)–S(6′), 3.733 Å (Fig. 3). The complex, however, does not form any further molecular interaction through S–S contacts in the solid state, which was observed for several $C_8H_4S_8$-metal complexes [4,11,12,36].

3.2. Electrochemical properties of complexes *1–7*

Fig. 4 shows cyclic voltammograms of **5** and **6** measured in dichloromethane. The coupled oxidation/reduction peak potentials at −0.02/−0.16 V (vs. Ag/Ag^+) observed for **6** seem to correspond to the first oxidation/reduction of the $C_8H_4S_8$ moiety, as described below. This complex exhibits also an oxidation peak potential at +0.21 V due to the second $C_8H_4S_8$-centered oxidation. Furthermore, the oxidation peak at +0.64 V is likely ascribed to the oxidation of the gold(I) ion. Complex **7** has exhibited similar oxidation potentials:

Table 3
Selected bond distances (Å) and angles (°) of $[(PEt_3)Au–C_3S_5–Au(PEt_3)]$ (**5**)

Au(1)–S(1)	2.320(2)	Au(1)–P(1)	2.261(2)
Au(2)–S(5)	2.337(2)	Au(2)–P(2)	2.265(2)
Au(1′)–S(1′)	2.305(2)	Au(2′)–P(1′)	2.254(2)
Au(2′)–S(5′)	2.327(2)	Au(2′)–P(2′)	2.261(2)
S(1)–C(1)	1.750(8)	S(2)–C(1)	1.754(7)
S(2)–C(2)	1.733(9)	S(3)–C(2)	1.662(8)
S(4)–C(2)	1.704(9)	S(4)–C(3)	1.745(7)
S(5)–C(3)	1.768(7)	S(1′)–C(1′)	1.742(8)
S(2′)–C(1′)	1.753(7)	S(2′)–C(2′)	1.701(9)
S(4′)–C(3′)	1.749(7)	S(5′)–C(3′)	1.754(7)
C(1)–C(3)	1.33(1)	C(1′)–C(3′)	1.34(1)
S(1)–Au(1)–P(1)	168.14(8)	S(5)–Au(2)–P(2)	175.64(7)
S(1′)–Au(1′)–P(1′)	163.35(8)	S(5′)–Au(2′)–P(2′)	177.08(8)
Au(1)–S(1)–C(1)	104.8(3)	C(1)–S(2)–C(2)	97.2(4)
C(2)–S(4)–C(3)	97.9(4)	Au(2)–S(5)–C(3)	102.3(2)
Au(1′)–S(1′)–C(1′)	105.6(3)	C(1′)–S(2′)–C(2′)	97.5(4)
C(2′)–S(4′)–C(3′)	98.4(4)	Au(2′)–S(5′)–C(3′)	104.5(2)
S(1)–C(1)–C(3)	129.0(6)	S(2)–C(1)–C(3)	115.7(6)
S(2)–C(2)–S(3)	123.4(5)	S(2)–C(2)–S(4)	112.9(4)
S(3)–C(2)–S(4)	123.7(5)	S(4)–C(3)–C(1)	116.3(6)
S(5)–C(3)–C(1)	128.5(6)	S(1′)–C(1′)–C(3′)	128.8(6)
S(2′)–C(1′)–C(3′)	116.6(6)	S(2′)–C(2′)–S(3′)	123.1(5)
S(2′)–C(2′)–S(4′)	113.2(5)	S(3′)–C(2′)–S(4′)	123.8(6)
S(4′)–C(3′)–C(1′)	114.3(5)	S(5′)–C(3′)–C(1′)	129.0(6)

Table 4
Selected bond distances (Å) and angles (°) of $[(PEt_3)Au–C_8H_4S_8–Au(PEt_3)]$ (**6**)

Au(1)–P(1)	2.2702(10)	Au(2)–P(2)	2.2623(10)
Au(1)–S(1)	2.3403(9)	Au(2)–S(8)	2.3389(10)
S(1)–C(1)	1.756(3)	S(2)–C(1)	1.773(3)
S(2)–C(2)	1.751(3)	S(3)–C(3)	1.757(4)
S(3)–C(4)	1.763(4)	S(4)–C(4)	1.750(4)
S(4)–C(5)	1.795(5)	S(5)–C(6)	1.772(6)
S(5)–C(7)	1.741(4)	S(6)–C(3)	1.769(4)
S(6)–C(7)	1.763(4)	S(7)–C(2)	1.767(4)
S(7)–C(8)	1.778(3)	S(8)–C(8)	1.743(4)
C(1)–C(8)	1.342(5)	C(2)–C(3)	1.333(5)
C(4)–C(7)	1.337(5)	C(5)–C(6)	1.431(8)
S(1)–Au(1)–P(1)	178.98(4)	S(8)–Au(2)–P(2)	164.47(4)
Au(1)–S(1)–C(1)	100.0(1)	C(1)–S(2)–C(2)	95.5(2)
C(3)–S(3)–C(4)	94.6(2)	C(4)–S(4)–C(5)	102.4(2)
C(6)–S(5)–C(7)	100.1(2)	C(3)–S(6)–C(7)	93.9(2)
C(2)–S(7)–C(8)	95.4(2)	Au(2)–S(8)–C(8)	104.3(1)
S(1)–C(1)–C(8)	127.4(3)	S(2)–C(1)–C(8)	117.1(2)
S(2)–C(2)–S(7)	113.4(2)	S(2)–C(2)–C(3)	123.4(3)
S(3)–C(3)–S(6)	113.8(2)	S(3)–C(3)–C(2)	123.1(3)
S(3)–C(4)–C(7)	116.7(3)	S(4)–C(4)–C(7)	128.8(3)
S(4)–C(5)–C(6)	118.6(4)	S(5)–C(6)–C(5)	117.5(4)
S(5)–C(7)–C(4)	127.5(3)	S(6)–C(7)–C(4)	117.9(3)
S(7)–C(8)–C(1)	116.4(2)	S(8)–C(8)–C(1)	130.2(3)

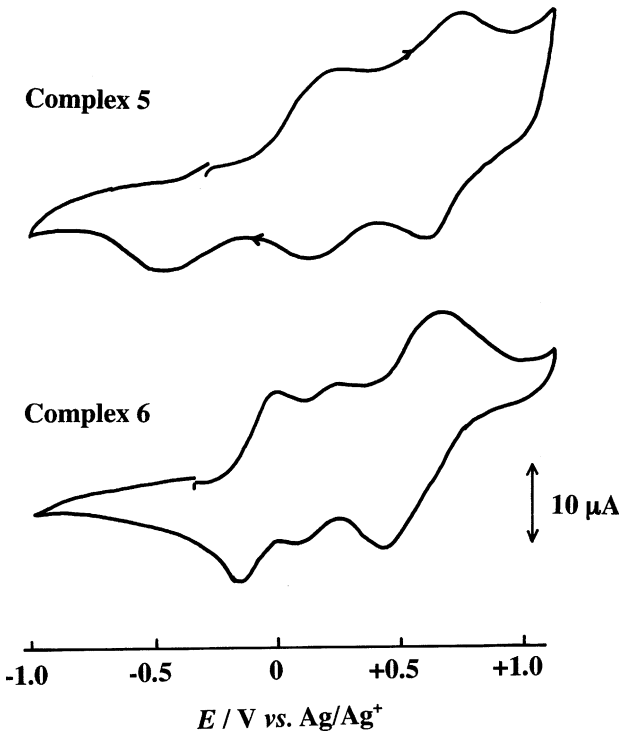

Fig. 4. Cyclic voltammograms of **5** and **6** (1.0×10^{-3} mol dm^{-3}) in dichloromethane. Supporting electrolyte: 0.1 mol dm^{-3} [NBu_4][ClO_4]. Sweep rate: 500 mV s^{-1}.

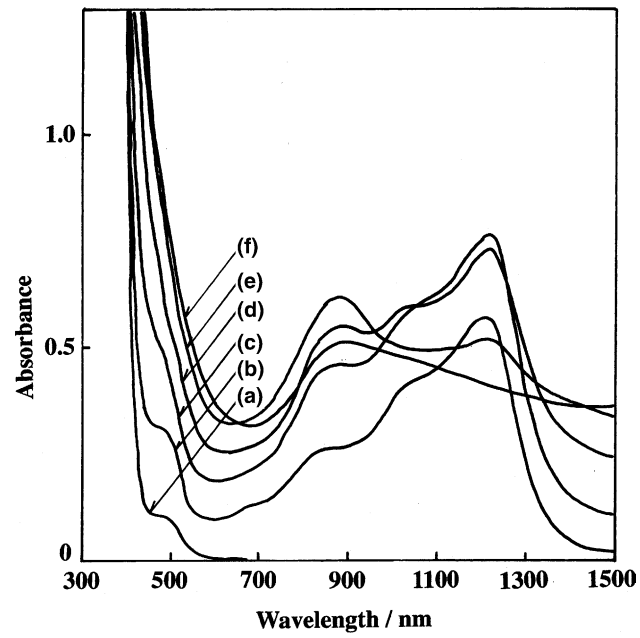

Fig. 5. Electronic absorption spectra of **7** (2.0×10^{-4} mol dm^{-3}) in dichloromethane in the presence of varying amounts of iodine: (a) 0, (b) 0.40×10^{-4}, (c) 0.80×10^{-4}, (d) 1.2×10^{-4}, (e) 1.6×10^{-4}, (f) 2.0×10^{-4} mol dm^{-3}.

−0.04, +0.23, and +0.65 V (vs. Ag/Ag$^+$). As shown in Fig. 4, complex **5** having the C_3S_5 moiety exhibits a rather higher, first oxidation potential at +0.22 V (vs. Ag/Ag$^+$) ascribed to the C_3S_5 moiety-centered oxidation, and the second oxidation occurs at +0.63 V.

The anionic complexes **1**–**4** exhibit further lower potentials for the C_3S_5- and $C_8H_4S_8$-centered oxidation than neutral species **5**–**7**. Oxidation potentials of the $C_8H_4S_8$-complexes [**3**: −0.29, −0.06 V, **4**: −0.30, −0.03 V (vs. Ag/Ag$^+$)] are lower than those of the C_3S_5-complexes [**1**: −0.16, +0.50 V, **2**: −0.05, +0.47 V]. The finding that the $C_8H_4S_8$-complexes show appreciably lower oxidation potentials than the corresponding C_3S_5-complexes was also observed for many C_3S_5- and $C_8H_4S_8$-metal complexes [4–7,22–26].

Thus, all these complexes having low oxidation potentials due to the ligand-centered oxidation can be oxidized by iodine and TCNQ.

3.3. Oxidation of complexes 1–5 and properties of the oxidized species 6–12

Electronic absorption spectra of complex **7** in dichloromethane in the presence of varying amounts of iodine as an oxidizing agent are shown in Fig. 5. The increase of amounts of iodine affords at first a band at 1200 nm, which is ascribed to the one-electron-oxidized species. Large deviation of base lines in the spectra with increasing amounts of iodine is due to the partial deposition of the oxidized species in solids because of the extreme low solubility. Further addition of iodine affords the band around 900 nm, which is assigned to the two-electron-oxidized species. The similar higher energy shift of ligand-metal charge transfer bands for the two-electron-oxidation of the $C_8H_4S_8$-ligand was observed for some $C_8H_4S_8$ and related sulfur-rich dithiolate-metal complexes [5,24,37].

Since **7** exhibits a low first oxidation potential, it may be oxidized even by TCNQ as a weak oxidizing agent. Fig. 6 shows the electronic absorption spectra of **7** in the presence of various amounts of TCNQ. Addition of TCNQ gives the intense band due to the TCNQ$^{\cdot-}$ radical anion around the 600–850 nm region [38] and a broad band around 1200 nm corresponds to the band shown in Fig. 5, which is ascribed to the one-electron-oxidized species. The observed band intensity of the TCNQ$^{\cdot-}$ radical anion is maximized by the addition of equivalent molar amount of TCNQ to **7**, indicating also the formation of one-electron-oxidized species of **7**.

Reactions of **3**, **6** and **7** with TCNQ have afforded essentially one-electron-oxidized species **15**–**17** containing the TCNQ$^{\cdot-}$ radical anion, which has been confirmed by IR ν(C≡N) absorption bands of 2192–2194 cm^{-1}. Powders of **15** have shown a sharp ESR signal at $g = 2.004$ (peak-to-peak linewidth, 1.4 mT). This indicates the $C_8H_4S_8$ ligand-centered oxidation, as observed for other oxidized $C_8H_4S_8$-metal complexes [4–6,22–26]. Complex **16** also has exhibited a sharp signal at

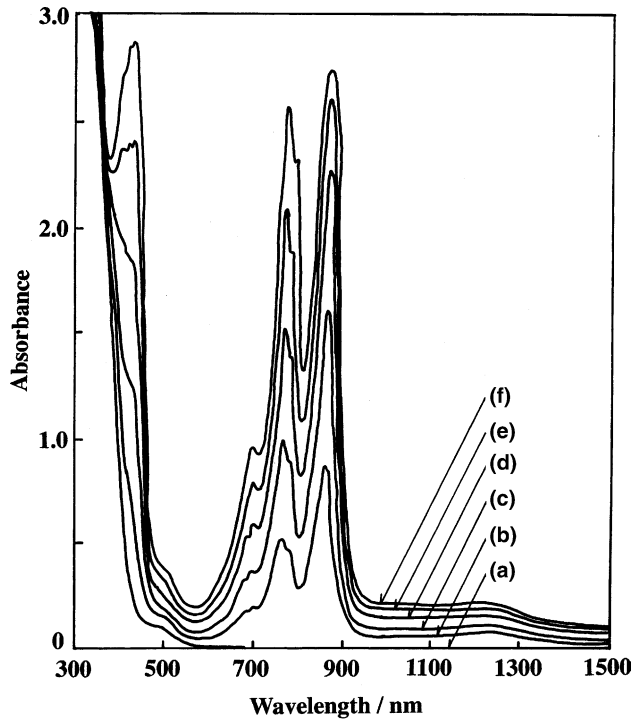

Fig. 6. Electronic absorption spectra of **7** (2.0×10^{-4} mol dm^{-3}) in dichloromethane in the presence of varying amounts of TCNQ: (a) 0, (b) 0.40×10^{-4}, (c) 0.80×10^{-4}, (d) 1.2×10^{-4}, (e) 1.6×10^{-4}, (f) 2.0×10^{-4} mol dm^{-3}.

$g = 2.002$ (peak-to-peak linewidth, 1.1 mT), indicating both the $C_8H_4S_8$ ligand moiety-centered oxidation and the TCNQ$^{\cdot-}$ radical anion. The binding energy of Au $4f_{1/2}$ electrons of **16** determined by XPS is 85.4 eV, which is similar to 84.9 eV for **6**. These findings confirm the Au(I) state and the $C_8H_4S_8$ ligand-centered oxidation for **16**.

Reactions of **1–4** with excess amounts of iodine in dichloromethane have afforded oxidized species **8–11**. They contain both I_3^- and I_5^- ions, which have been confirmed by two Raman bands observed at 112 and 164 cm^{-1}, assigned to stretching modes of I_3^- and I_5^- ions, respectively [39,40], for **11**. Thus, these oxidized species are in an over one-electron-oxidized state. Complex **11** has exhibited almost an isotropic ESR signal at $g = 2.006$ (peak-to-peak linewidth, 3.3 mT). And it has shown an IR absorption band at 1271 cm^{-1} ascribed to one of the C=C bonds of the $C_8H_4S_8$ moiety, which is lower than that (1286 cm^{-1}) of the unoxidized species **4**. These findings indicate the $C_8H_4S_8$-centered oxidation for **11**. Complexes **8–10** also have similar ESR spectra. Furthermore, the binding energy of Au $4f_{1/2}$ electrons of **11** has been determined to be 86.1 eV, which is larger by 1.6 eV than that of the unoxidized species **4**. These findings suggest the Au(III) state for **11**.

For the dinuclear neutral complexes **5–7**, the reactions with excess amounts of iodine in dichloromethane have yielded oxidized species **12–14**. They have also

Table 5
Electrical conductivities (σ)[a] of the oxidized complexes

Complex	σ_{RT} (S cm^{-1})
8	3.0×10^{-4}
9	5.1×10^{-7}
10	2.1×10^{-2}
11	3.2×10^{-2}
12	5.1×10^{-8}
13	1.4×10^{-4}
14	3.5×10^{-3}
15	1.8×10^{-3}
16	1.9×10^{-4}
17	5.7×10^{-3}

[a] Measured for compacted pellets at room temperature.

both I_3^- and I_5^- ions as the counter anion, which have been confirmed by two Raman bands observed at 111 and 163 cm^{-1} for **13**. This complex has also shown an almost isotropic ESR signal at $g = 2.004$ (peak-to-peak linewidth, 5.0 mT), and the binding energy of Au $4f_{1/2}$ electrons (86.4 eV) is larger than that (84.9 eV) of the unoxidized species **6**. Thus, these oxidized complexes are likely to have the $C_8H_4S_8$-centered oxidation and the Au(III) state, as deduced for **8–11**.

Complexes **1–7** are essentially insulators with electrical conductivities of $<10^{-9}$ S cm^{-1} measured for compacted pellets at room temperature. The oxidized complexes **8–17** behave as electrical conductors and their electrical conductivities are listed in Table 5. The oxidized C_3S_5-complexes **9** and **12** exhibit low electrical conductivities as reported for other oxidized C_3S_5-metal complexes [36,41], except for **8** showing the conductivity of 3.0×10^{-4} S cm^{-1}. On the other hand, the oxidized $C_8H_4S_8$-complexes **10**, **11**, **13–17** exhibit considerably high conductivities (1.4×10^{-4}–3.2×10^{-2} S cm^{-1}). Especially, **10** and **11** behave as good electrical conductors. Even in the bulky $C_8H_4S_8$-metal complexes having PEt_3 and PPh_3, effective S–S non-bonded contacts among the oxidized dithiolate ligand moieties are likely to occur in the solid state, as observed for other oxidized $C_8H_4S_8$-metal complexes having bulky groups [5,6,37,42].

Acknowledgements

We are grateful to Professor S. Suzuki (Graduate School of Science, Osaka University) for the measurement of ESR spectra and to Professor R. Arakawa (Faculty of Engineering, Kansai University) for the measurement of electrospray mass spectra. This research was supported in part by Grant-in-aids for Scientific Research (Nos. 13029071 and 14044056) from Ministry of Education, Science, Sports and Culture, Japan and by a Strategic Research Base Upbringing Special Coordination Fund for Promoting Science and Technology.

References

[1] P. Cassoux, L. Valade, K. Kobayashi, A. Kobayashi, R.A. Clark, A.E. Underhill, Coord. Chem. Rev. 110 (1991) 115.
[2] R.-M. Olk, B. Olk, W. Dietzsch, R. Kirmse, E. Hoyer, Coord. Chem. Rev. 117 (1992) 99.
[3] A.E. Allen, R.-M. Olk, Coord. Chem. Rev. 188 (1999) 211.
[4] G. Matsubayashi, M. Nakano, H. Tamura, Coord. Chem. Rev. 226 (2002) 143.
[5] H. Mori, M. Nakano, H. Tamura, G. Matsubayashi, J. Organomet. Chem. 574 (1999) 77.
[6] K. Saito, M. Nakano, H. Tamura, G. Matsubayashi, Inorg. Chem. 39 (2000) 4815.
[7] G. Matsubayashi, M. Nakano, K. Saito, T. Yonamine, R. Arakawa, J. Organomet. Chem. 611 (2000) 364.
[8] G. Matsubayashi, A. Yokozawa, J. Chem. Soc. Dalton Trans. (1990) 3535.
[9] M. Nakano, A. Kuroda, T. Maikawa, G. Matsubayashi, Mol. Cryst. Liq. Cryst. 284 (1996) 301.
[10] M. Nakano, A. Kuroda, G. Matsubayashi, Inorg. Chim. Acta 254 (1997) 189.
[11] K. Kubo, M. Nakano, H. Tamura, G. Matsubayashi, M. Nakamoto, J. Organomet. Chem. 669 (2003) 141.
[12] K. Kubo, M. Nakano, H. Tamura, G. Matsubayashi, Eur. J. Inorg. Chem. (2003) 4093.
[13] M. Nakamoto, A. Schier, H. Schmidbaur, J. Chem. Soc. Dalton Trans. (1993) 1341.
[14] M. Nakamoto, W. Hiller, H. Schmidbaur, Chem. Ber. 126 (1993) 605.
[15] R.M. Davila, R.J. Staples, A. Elduque, M.M. Harlass, L. Kyle, J.P. Fackler Jr., Inorg. Chem. 33 (1994) 5940.
[16] E. Cerrada, A. Laguna, M. Laguna, P.G. Jones, J. Chem. Soc. Dalton Trans. (1994) 1325.
[17] E. Cerrada, P.G. Jones, A. Laguna, M. Laguna, Inorg. Chem. 35 (1996) 2995.
[18] E. Cerrada, P.G. Jones, A. Laguna, M. Laguna, Inorg. Chim. Acta 249 (1996) 163.
[19] G. Steimecke, H.J. Sieler, R. Kirmse, E. Hoyer, Phosphorus Sulfur 7 (1979) 49.
[20] N. Svenstrup, K.M. Rasmussen, T.K. Kansen, J. Becher, Synthesis (1994) 809.
[21] L. Binet, J.M. Fabre, C. Montginoul, K.B. Simonsen, J. Becher, J. Chem. Soc. Perkin Trans. 1 (1996) 783.
[22] M. Nakano, A. Kuroda, H. Tamura, R. Arakawa, G. Matsubayashi, Inorg. Chim. Acta 279 (1998) 165.
[23] K. Natsuaki, M. Nakano, G. Matsubayashi, Inorg. Chim. Acta 299 (2000) 112.
[24] T. Nakazono, M. Nakano, H. Tamura, G. Matsubayashi, J. Mater. Chem. 9 (1999) 2313.
[25] K. Kubo, M. Nakano, G. Matsubayashi, Inorg. Chim. Acta 346 (2003) 43.
[26] A. Nakahama, M. Nakano, G. Matsubayashi, Inorg. Chim. Acta 284 (1999) 55.
[27] T. Higashi, ABSCOR Program for absorption correction, Rigaku Corporation, Tokyo, Japan, 1995.
[28] M. Sheldrick, SHELX86 Program for the solution of crystal structure, University of Gottingen, Germany, 1985.
[29] Altomare, G. Cascarano, C. Giacovazzo, A. Guagliardi, M.C. Burla, G. Polidori, M. Camalli, J. Appl. Cryst. 27 (1994) 435.
[30] G.M. Sheldrick, SHELXL97 Program of the refinement of crystal structure, University of Gottingen, Germany, 1997.
[31] International Tables for X-Ray Crystallography, vol. 4, Kynoch Press, Birmingham, England.
[32] C.K. Johnson, ORTEP-II, Report ORNL-5138, Oak Ridge National Laboratory, Oak Ridge, TN, 1976, p. 435.
[33] M. Davila, R.J. Staples, A. Elduque, M.M. Harlass, L. Kyle, J.P. Fackler Jr., Inorg. Chem. 32 (1993) 1749.
[34] M.C. Gimeno, P.G. Jones, A. Laguna, M. Laguna, R. Terroba, Inorg. Chem. 33 (1994) 3932.
[35] R.M. Davila, R.J. Staples, A. Elduque, M.M. Harlass, L. Kyle, J.P. Fackler Jr., Inorg. Chem. 33 (1994) 5940.
[36] K. Kubo, M. Nakano, H. Tamura, G. Matsubayashi, Inorg. Chim. Acta 336 (2002) 120.
[37] G. Matsubayashi, T. Ryowa, H. Tamura, M. Nakano, R. Arakawa, J. Organomet. Chem. 645 (2002) 94.
[38] J. Tanaka, M. Tanaka, T. Kawai, T. Takabe, O. Maki, Bull. Chem. Soc. Jpn. 49 (1976) 2358.
[39] M. Cowie, A. Gleizes, G.W. Grynkewich, D.W. Kalina, M.S. McClure, R.P. Scaringe, R.C. Teitelbaum, S.L. Ruby, J.A. Ibers, C.R. Kannewurf, T.J. Marks, J. Am. Chem. Soc. 101 (1979) 2921.
[40] B.N. Diel, T. Inabe, J.W. Lyding, K.F. Schoch Jr., C.R. Kannewurf, T.J. Marks, J. Am. Chem. Soc. 105 (1983) 1551.
[41] G. Matsubayashi, M. Hirao, T. Tanaka, Inorg. Chim. Acta 144 (1988) 217.
[42] K. Saito, M. Nakano, H. Tamura, G. Matsubayashi, J. Organomet. Chem. 625 (2001) 7.